LINEAR THEORY OF AN ELECTRON CYCLOTRON MASER OPERATING AT THE FUNDAMENTAL

K. E. Kreischer, R. J. Temkin

March 1980

PFC/JA-80-6

LINEAR THEORY OF AN ELECTRON CYCLOTRON MASER OPERATING AT THE FUNDAMENTAL *

K. E. Kreischer, R. J. Temkin

Plasma Fusion Center† and National Magnet Laboratory**
Massachusetts Institute of Technology
Cambridge, Massachusetts 02139

* Work supported by U.S.D.O.E. Contract DE-AC-02-80ER52059

† Supported by U.S. Department of Energy

** Supported by National Science Foundation

Abstract

The linear theory of an electron cyclotron maser (ECM) operating at the fundamental is developed. A set of analytic expressions, valid for all TE cavity modes, is derived for the starting current and frequency detuning using the Vlasov-Maxwell equations in the weakly relativistic limit. These results are applicable for an arbitrary electron velocity distribution as well as any longitudinal distribution of the RF field. It is shown that the starting current can be expressed in a simple form which contains the Fourier transform of the longitudinal field distribution. Analytic results are presented for specific longitudinal field variations, including uniform, sinusoidal, and Gaussian. It is found that the starting characteristics of an ECM are strongly influenced by the axial dependence of the RF field, but weakly affected by the velocity spread of the electron beam. The problem of multimode oscillation is treated in the linear theory by using a Slater expansion of the cavity field. The complete formulation for mode competition based on this expansion is presented and preliminary results are derived. This comprehensive analysis of ECM linear theory should be useful as a diagnostic of ECM performance and should facilitate comparison between theory and experiment.

I. Introduction

The electron cyclotron resonance maser (ECM) has been demonstrated to be an efficient, high power source of millimeter and submillimeter radiation [1-3]. The most successful results to date have been obtained with a form of the maser called the gyrotron, developed by A. V. Gaponov and co-workers [1]. In this paper we present new results in the linear theory of the ECM, results which are particularly applicable to the gyrotron.

The linear theory of the ECM describes the characteristics of the maser at threshold, including the starting current I_{ST} and the detuning of the operating frequency from the empty cavity resonance frequency. In general, linear theory results may be expressed in analytic form, as is the case in this work. In contrast, the nonlinear theory, which describes the operation of the maser above threshold and yields the output power and efficiency of the device, must ordinarily be solved numerically. The linear theory provides a simple means of determining the threshold operating characteristics of an ECM, making it an important tool in the analysis of this device.

There have been a number of previous investigations of the linear theory of the ECM [4-9]. However, these studies have been limited or idealized in one respect or another, such as by treating only specific cavity modes or electron beams with no velocity spread. In this paper we present an analytic treatment of ECM linear theory that is applicable to all TE modes of the cavity, as well as to an arbitrary, weakly relativistic, electron velocity distribution.

Furthermore, the results presented are valid for any distribution of the longitudinal RF field. This allows one to compare the linear characteristics of different models of an ECM cavity, including: an idealized right circular cylinder cavity with closed ends and sinusoidal longitudinal RF field; and a more realistic cavity with open ends and a Gaussian distribution. In addition, the present comprehensive results enable us to evaluate important effects in the ECM, including mode competition and the changes caused by a velocity spread in the electron beam. By analyzing these effects, we are better able to determine what factors can strongly influence the threshold behavior of an ECM. This should facilitate the comparison between theoretical and experimental results and serve as a useful aid in diagnosing ECM performance.

The method employed in this analysis involves solving the combined Vlasov and Maxwell equations for an electron beam interacting with the RF fields of a cavity. The Vlasov equation is solved by a standard perturbation approach in the weakly relativistic limit. The results are then combined with the Slater equations for the cavity modes and solved for the oscillation condition. This yields expressions for both the starting current and the frequency detuning. Calculation of the starting current allows one to determine the minimum beam current needed for self-oscillation. The frequency detuning, which depends on the cavity Q, may provide a means of determining Q experimentally by measuring the resonance frequency of the cavity both with and without the electron beam present.

Our analysis is presented in the following manner. In Section II, the problem is formulated and general expressions for the starting current and frequency detuning are presented. In Section III, these results are applied to three different longitudinal RF field profiles: uniform, sinusoidal, and Gaussian. This comparison allows one to determine how sensitive the threshold behavior of an ECM is to the field structure. Section IV discusses the effect of introducing a velocity spread into the electron beam, while Section V investigates the problems associated with multimoding. Conclusions are presented in Section VI.

II. General Theory

The formulation used for describing the ECM consists of a combination of the Vlasov equation for the electron distribution function and Maxwell equations for the RF cavity fields. A number of assumptions are made that aid in simplifying the calculation without severely limiting its usefulness. We are concerned with the small signal (i.e., linear) operation of an ECM. The cavity is assumed to have a cross-sectional shape that is uniform or slowly varying along its axis, here chosen as the z-axis. This allows us to solve the Helmholtz equation, which describes the field structure within the cavity, by a separation of variables. The RF field can then be expressed as a product of two functions, one describing the cross-sectional structure and the other giving the field variation along z. Space charge effects are neglected. The electron beam is assumed to be weakly relativistic, with relativistic effects included in the calculation by retaining the velocity dependence of the electron mass m_e and the cyclotron frequency ω_c. The dependence of ω_c on velocity is crucial in order for emission to occur. Finite Larmor radius effects are neglected, and as a consequence the results presented in this paper are applicable only to an ECM operating at the fundamental frequency, i.e., $\omega \simeq \omega_c$.

This calculation will include only the interaction between the beam and the RF electric field, and will neglect the RF magnetic field. Results from a previous paper [9] indicate that the terms associated with the magnetic field are small if $\omega_c/k_{||} c \gg 1$, where

$k_{||}$ is the wavenumber parallel to the z-axis. Since a gyrotron operates near cutoff and satisfies the above inequality, this paper is especially applicable to this device. This same condition also results in TE modes having substantially higher gain than TM modes, and for this reason the latter will not be treated in this paper.

The initial electron distribution function is assumed to be separable into a product of two distributions, one in velocity space and one in real space:

$$f_o(\bar{r},\bar{v},t = 0) = N(r,\theta)f_o(u,w) \tag{1}$$

where

$$2\pi \int_{-\infty}^{\infty} du \int_{o}^{\infty} wdw\ f_o(u,w) = 1$$

Here, $f_o(u,w)$ is expressed in terms of the electron velocities parallel and perpendicular to the z-axis, u and w respectively. $N(r,\theta)$ is the spatial density of the beam, and is expressed in terms of the cylindrical coordinates r and θ, but is independent of z. It has recently been shown [8,17] that this assumption of separability in Eq.(1) is generally not valid unless $w/\omega_c r_e << 1$, where r_e is the beam radius. Hence, we also implicitly assume this latter condition.

We begin with a Slater expansion [10] of the RF vacuum field within the cavity:

$$\bar{E}(\bar{r},t) = \sum_{\ell} p_\ell(t)\bar{E}_\ell(\bar{r})$$
$$\bar{H}(\bar{r},t) = \sum_{\ell} q_\ell(t)\bar{H}_\ell(\bar{r}) \tag{2}$$

where the field components have been written as sums of orthonormal modes that satisfy:

$$\int_V d^3r\ \bar{E}_\ell \cdot \bar{E}_d = \int_V d^3r\ \bar{H}_\ell \cdot \bar{H}_d = \delta_{\ell d}$$

Here, V is the cavity volume, $\omega_\ell = ck_\ell$ is the vacuum frequency of the mode, and $p_\ell(t)$ and $q_\ell(t)$ describe the amplitudes and time dependences of the field components. Writing Maxwell's equations $\nabla \times \bar{E} = -\mu_o \partial\bar{H}/\partial t$ and $\nabla \times \bar{H} = \bar{J} + \varepsilon_o \partial\bar{E}/\partial t$ in terms of the above expansions, combining these two equations, and utilizing the orthogonal characteristics of $\bar{E}_\ell$ and $\bar{H}_\ell$ leads to an expression describing the time-dependent behavior of the ℓ^{th} mode [10]:

$$\frac{1}{c^2}\ \frac{d^2p_\ell}{dt^2} + k_\ell^2\ \bar{p}_\ell = -\mu_o \frac{d}{dt}\left(\int_V d^3r\, \bar{J}\cdot\bar{E}_\ell - \int_{S'} dA(\hat{n} \times \bar{H})\cdot\bar{E}_\ell \right) - k_\ell \int_S dA\ (\hat{n} \times \bar{E})\cdot\bar{H}_\ell \qquad (3)$$

where $\hat{n}$ is a vector normal to the cavity surface and pointing outward. The multimode nature of this problem is embodied in the fact that $\bar{J}$,$\bar{E}$, and $\bar{H}$ must be expanded in terms of all possible cavity modes.

The surfaces S and S' represent two types of boundary conditions that are present. The S surface corresponds to the conducting walls of the cavity at which the tangential component of $\bar{E}$ is virtually zero. The S' surface corresponds to an insulated area and is associated with power coupled out of the cavity. The S integral can be rewritten in terms of the ohmic quality factor of the cavity, Q_o, by noting that $\hat{n} \times \bar{E} = \bar{H}(1 + i)\sqrt{\omega\mu_o/2\sigma}$ at a wall with conductivity σ. Using the following definition for $Q_o^{\ell d}$:

$$Q_o^{\ell d} = \sqrt{2\omega\sigma\mu_o}\left(\int_S dA\ \bar{H}_\ell\cdot\bar{H}_d \right)^{-1}$$

the S integral in Eq.(3) can be written as:

$$\int_S dA(\hat{n} \times \bar{E})\cdot\bar{H}_\ell = (i - 1) \sum_d \left(\frac{k_d}{Q_o^{\ell d}}\right) P_d \tag{4}$$

Here we have assumed that $Q_o^{\ell d} >> 1$ and have dropped terms of order $(Q_o^{\ell d})^{-2}$. The terms associated with $Q_o^{\ell d}$, $d \neq \ell$, which represent coupling between cavity modes, are typically small in a gryotron and can be neglected.

The S' integral can be expressed in terms of the diffractive Q, Q_D, that results from the output coupling of the cavity mode:

$$\int_{S'} dA(\hat{n} \times \bar{H})\cdot\bar{E}_\ell = - \varepsilon_o \left(\frac{\omega_\ell}{Q_D^\ell}\right) P_\ell \tag{5}$$

The superscript on Q_D indicates that this parameter is defined in terms of the stored energy in the ℓ^{th} mode and the power coupling between the ℓ^{th} mode of the cavity and the output mode of the waveguide connected to the cavity. No mode coupling terms are obtained from this integral. Combining Eqs.(3), (4), and (5) leads to the following result:

$$\frac{1}{c^2}\frac{d^2 P_\ell}{dt^2} + k_\ell^2 P_\ell = - \mu_o \frac{d}{dt}\left[\int_v d^3 r \bar{J}\cdot\bar{E}_\ell + \varepsilon_o\left(\frac{\omega_\ell}{Q_D^\ell}\right) P_\ell\right]$$

$$- (i - 1)\left(\frac{k_\ell^2}{Q_o^{\ell\ell}}\right) P_\ell \tag{6}$$

If an equilibrium exists within the cavity, it is possible to express this equation as two separate relations, one describing the energy balance within the cavity while the other determines the frequency detuning. Writing $p_\ell = p_{o\ell}\exp[i\omega(\ell)t]$, where $p_{o\ell}$ is independent of time, the decoupled expressions are:

$$\left(\frac{\omega_\ell}{Q_T^\ell}\right) = -\frac{1}{\varepsilon_o}\,\mathrm{Re}\left[\frac{1}{p_{o\ell}}\int_v d^3r\ \bar{J}\cdot\bar{E}_\ell\right] \tag{7a}$$

$$\left(\omega'_\ell\right)^2 - \left(\omega(\ell)\right)^2 = \frac{\omega(\ell)}{\varepsilon_o}\,\mathrm{Im}\left[\frac{1}{p_{o\ell}}\int_v d^3r\ \bar{J}\cdot\bar{E}_\ell\right] \tag{7b}$$

where

$$Q_T^\ell = \frac{Q_D^\ell\, Q_o^{\ell\ell}}{Q_D^\ell + Q_o^{\ell\ell}}$$

$$\omega'_\ell = \omega_\ell\sqrt{1 - (Q_o^{\ell\ell})^{-1}}$$

Here Q_T^ℓ is the overall quality factor, and $\omega(\ell)$ is the operating frequency of the ℓ^{th} mode, which generally differs from ω_ℓ.

If we have a cylindrical cavity with no taper and an arbitrary cross section, then the electric field of a single TE mode in equilibrium can be written as [20]:

$$\bar{E}(\bar{r},t) = \bar{T}(r,\theta)g(z)\exp(i\omega t) \tag{8}$$

where $\bar{T}(r,\theta)$ and $g(z)$ satisfy:

$$\bar{T}(r,\theta) = \hat{z} \times \nabla_\perp \Psi$$

$$d^2g(z)/dz^2 + k_{||}^2\, g(z) = 0 \qquad (9)$$

$$k_\perp^2 + k_{||}^2 = \omega^2/c^2$$

$$\nabla_\perp^2 \Psi + k_\perp^2 \Psi = 0$$

Here $\hat{z}$ is a unit vector, Ψ is determined by the boundary conditions, and $k_\perp$ and $k_{||}$ are constants. $\bar{T}(r,\theta)$ gives the field amplitude and cross-sectional structure, and can be complex, while $g(z)$ is real and describes the longitudinal field profile. In this paper $g(z)$ is normalized to a maximum value of one. It can be shown that Eqs.(8) and (9) also apply to cavities with weakly irregular features at the ends for output coupling, or with slowly tapered cross sections, if we allow $k_\perp$, $k_{||}$, and Ψ to become functions of z [11,21]. The dependence of $\bar{T}$ on z will be relatively weak for these cavities, and can be neglected.

An expression can be obtained for $P_{o\ell}$ by equating Eqs.(2) and (8), squaring and integrating over the cavity volume. This gives:

$$|P_{o\ell}|^2 = \int_V d^3r\, |g_\ell(z)\, \bar{T}_\ell(r,\theta)|^2 \qquad (10)$$

The parameter $p_{o\ell}$ serves as a normalization factor in Eqs.(7) so that, in a single mode analysis, the starting current and detuning are independent of field amplitude. Also noteworthy is the fact that $(\varepsilon_o p_{o\ell}^2/2)$ is equal to the total stored energy (electric plus magnetic RF fields) within the cavity in the ℓ^{th} mode.

Equations for Single Mode Operation

We must now solve the integrals in Eqs.(7). In general, $\bar{J}$ is written in terms of all modes existing within the cavity. However, we will initially limit our attention to a single oscillating TE mode and leave the discussion of multimoding to a later section. Starting with the linearized Vlasov and Maxwell equations, the perturbation $f_1(\bar{r},\bar{v},t)$ of the distribution function of the electron beam due to the RF electric field in the cavity can be calculated using the method of characteristics [13]. This method is appropriate as long as the perturbation is small, that is, the field amplitude is small. An expression for $\bar{J}$ can be derived based on this perturbed distribution. The approach followed is a standard perturbation method [4,8] so that we will only present the final results. The integrals of Eqs.(7) can be expressed in the following form:

$$\frac{1}{P_{o\ell}}\int_v d^3r\ \bar{J}\cdot\bar{E}_\ell = \frac{-e}{P_{o\ell}}\int_v d^3r\ N(r,\theta)\int d^3v\ \bar{E}_\ell\cdot\bar{v}\ f_1(\bar{r},\bar{v},t)$$

$$= |P_{o\ell}|^{-2}\ \frac{e^2}{m_e}\frac{\pi}{k_{\|}^2}\int_{-\infty}^{\infty} du\int_o^{\infty} dw\ f_o(u,w)\left(\frac{w}{u}\right)\left[1 - \frac{1}{2}\left(\frac{sw^2}{c^2}\right)\ \frac{d}{dx}\right]$$

$$X\left[(F_c^{\ell\ell} + i\ F_s^{\ell\ell})(G_D^{\ell\ell} - iG_c^{\ell\ell})\right] \qquad (11)$$

where

$$G_D^{\ell d} = \int_o^{2\pi} d\theta \int_o^{r_w} r\ dr\ N(r,\theta)(\bar{T}_\ell\cdot\bar{T}_d^*)$$

$$G_C^{\ell d} = \int_o^{2\pi} d\theta \int_o^{r_w} r\, dr\, N(r,\theta) \left| \bar{T}_\ell \times \bar{T}_d^* \right|$$

$$x_\ell = \frac{\left[\omega_c - \omega(\ell)\right]}{k_{||}\, u}$$

$$s = \frac{\omega_c}{k_{||}\, u}$$

$$\omega_c = \frac{eB}{m_e c}$$

$$m_e = \gamma m_{eo}$$

Here, m_e is the relativistic electron mass, r_w is the cavity radius, and e is the electron charge. The strength of the interaction between the beam and the RF field is measured by the geometric factors G_D and G_C. The expression $\left[1 - 1/2(sw^2/c^2)d/dx\right]$ operates on the functions $F_c^{\ell\ell}$ and $F_s^{\ell\ell}$. These functions are determined by the longitudinal field dependence g(z), and can be calculated from the following equations:

$$F_c^{\ell d}(x_d) = \int_{-\infty}^{\infty} d\tilde{z} g_\ell(\tilde{z}) \int_o^{\infty} d\lambda g_d(\tilde{z} - \lambda) \cos(\lambda x_d) \qquad (12a)$$

$$F_s^{\ell d}(x_d) = \int_{-\infty}^{\infty} d\tilde{z} g_\ell(\tilde{z}) \int_o^{\infty} d\lambda g_d(\tilde{z} - \lambda) \sin(\lambda x_d) \qquad (12b)$$

where $\tilde{z} = k_{||}\, z$. In the next section, we will present detailed results for specific g(z) distributions. The derivative in Eq.(11) results

from the dependence of m_e, and consequently ω_c, on velocity, and is a measure of the electron bunching process.

We will now specialize to an annular electron beam that is symmetric in θ, has no radial thickness, and is located at $r = r_e$. We will limit our attention to an RF field with a standing wave structure in the θ direction, so that $\bar{T}_\ell$ is real and $G_c^{\ell\ell}$ is zero. Relating N to the beam current I, the geometric factor $G_D^{\ell\ell}$ can be written as:

$$G_D^{\ell\ell} = (I/e\bar{u})G(r_e)$$

where (13)

$$G(r_e) = \frac{1}{2\pi}\int_0^{2\pi} d\theta \; |\bar{T}_\ell(r_e,\theta)|^2$$

and $\bar{u}$ is the average longitudinal velocity. An explicit expression can now be written for the starting current I_{ST} by combining Eqs.(7a), (11), and (13). For clarity, the ℓ script has been dropped from all parameters except frequencies:

$$I_{ST} = -\epsilon_o \frac{\omega_\ell}{Q_T} |p_o|^2 \frac{m_e}{e} \frac{k_{||}^2 \bar{u}}{\pi G(r_e)} \left\{ \int_{-\infty}^{\infty} du \int_o^{\infty} dw \; f_o(u,w)\left(\frac{w}{u}\right)\left[F_c - \frac{1}{2}\left(\frac{sw^2}{c^2}\right)\frac{dF_c}{dx}\right]\right\}^{-1} \tag{14}$$

The starting current is positive and emission is possible only when $(sw^2/c^2)(F_c)^{-1}(dF_c/dx) > 2$.

A simple expression can also be obtained for the frequency detuning by dividing (7b) by (7a). Defining $y \equiv (\omega_c - \omega_\ell)(k_{||}\, u)^{-1}$ and assuming $|\omega_c - \omega_\ell| << \omega_\ell$, one can write:

$$\left(\frac{2Q_T}{s}\right)\left(y - x + \frac{s}{2Q_o} - \frac{y}{2Q_o}\right) = \frac{\int_{-\infty}^{\infty} du \int_0^{\infty} dw f_o(u,w)\left(\frac{w}{u}\right)\left[F_S - \frac{1}{2}\left(\frac{sw^2}{c^2}\right)\frac{dF_s}{dx}\right]}{\int_{-\infty}^{\infty} du \int_0^{\infty} dw f_o(u,w)\left(\frac{w}{u}\right)\left[F_c - \frac{1}{2}\left(\frac{sw^2}{c^2}\right)\frac{dF_c}{dx}\right]} \quad (15)$$

Eqs.(14) and (15) can be further simplified by assuming that the electron beam has no velocity spread and f_o can be represented by delta functions: $f_o(u,w) = (2\pi w_o)^{-1}\,\delta(u - u_o)\,\delta(w - w_o)$. This leads to the following set of equations:

$$I_{ST} = -2\varepsilon_o \frac{\omega_\ell}{Q_T} |p_o|^2 \frac{m_e}{e} \frac{(k_{\|} u_o)^2}{G(r_e)} \left[F_c - \frac{1}{2}\left(\frac{sw_o^2}{c^2}\right)\frac{dF_c}{dx}\right]^{-1} \quad (16a)$$

$$\left(\frac{2Q_T}{s}\right)\left(y - x + \frac{s}{2Q_o}\right) = \frac{F_s - \frac{1}{2}\left(\frac{sw_o^2}{c^2}\right)\frac{dF_s}{dx}}{F_c - \frac{1}{2}\left(\frac{sw_o^2}{c^2}\right)\frac{dF_c}{dx}} \quad (16b)$$

Note that I_{ST} is independent of the field amplitude, as is expected in linear theory. The term $y/2Q_o$ has been dropped in Eq.(16b) since it is very small in comparison to the other terms.

It can be seen that F_c and F_s, which are defined by Eq.(12), are crucial in determining the characteristics of the starting current and detuning. A simple expression can be obtained for F_c by writing it in terms of the Fourier transform of $g(\tilde{z})$. Using the transform:

$$\mathfrak{L}(k) = (2\pi)^{-\frac{1}{2}} \int_{-\infty}^{\infty} g(a)\, e^{ika}\, da$$

in conjunction with Eq.(12a) gives the following simple result:

$$F_c = \pi \mathcal{L}_\ell(x)\, \mathcal{L}^*_\ell(x) \tag{17}$$

Using Eq.(11), we have shown that F_s may be expressed in terms of F_c using the Kramers-Kronig relations [18]:

$$F_s = \pi^{-1} P \int_{-\infty}^{\infty} \frac{F_c(a)}{x-a}\, da \tag{18}$$

where P indicates the principal value of the integral. These two equations, in conjunction with (16), provide a convenient means of quickly determining the linear characteristics of an ECM. Moreover, because of the simple nature of these expressions, the possibility exists of defining the desired linear characteristics of an ECM, and then calculating the appropriate longitudinal field structure via these relations.

The functions $F_c(x)$ and $F_s(x)$ are very similar to the absorption and dispersion functions of a forced harmonic oscillator. Thus, it is possible to model the ECM interaction as a harmonic oscillator with natural frequency ω_c and a driving force due to the RF field with frequency ω. The damping time τ_d, which is inversely related to the resonance width, can be shown to be approximately equal to the time of interaction between the beam and RF field, $\tau_i \sim L/u$. If $\omega \neq \omega_c$, then the electron will precess with respect to the field, experiencing alternating periods of acceleration and deceleration. If the interaction continues indefinitely, ($\tau_i \to \infty$), then the net

electron energy change will be zero. In this case, an energy transfer to the electrons will occur only at $\omega = \omega_c$, and the resonance curve becomes a delta function located at $\omega = \omega_c$. However, if τ_i is finite, the periods of acceleration and deceleration will not exactly cancel for $\omega \neq \omega_c$, and the resonance curve will be broadened. The relationship between τ_d and τ_i can also be shown by noting that $F_c(x)$ typically has a width $\Delta x \sim 2$. Thus one can write:

$$\tau_d^{-1} = \frac{\Delta\omega}{2\pi} \simeq \frac{2k_{\parallel} u}{2\pi} = \frac{u}{L} = \tau_i^{-1}$$

This broadening mechanism is often called transit time broadening.

III. Results for Specific Cavity Field Structures

We will now apply the general theory for single mode oscillation given in Section II to specific longitudinal field structures. This comparison will allow us to determine the sensitivity of the linear characteristics of an ECM to g(z). We will consider a gyrotron that has a cavity of length L with a circular cross section. The cavity will either be uniform, or have a slow taper in the z direction, depending upon the nature of the output coupling and g(z). We will assume an annular electron beam located at $r = r_e$. Based on these assumptions, and assuming a standing wave in the θ direction, the starting current and frequency detuning are given in the case of a beam with a velocity spread by Eqs. (14) and (15) respectively, and in the case of no velocity spread by Eq. (16).

We will be considering three specific longitudinal field structures: sinusoidal, Gaussian, and uniform. A sinusoidal distribution is associated with a nontapered cavity with conducting walls at each end (at z=0 and L). In reality, a sinusoidal description for g(z) is generally not adequate since an ECM normally consists of an open resonator in which the field, rather than ending abruptly, extends beyond the ends of the cavity in order to achieve output coupling. In this case, g(z) can be calculated using Eq. (9) with $k_{||}$ a function of z, and is no longer necessarily of the form $\sin(k_{||} z)$. One approximation for g(z) is a Gaussian distribution, which serves as a reasonably accurate fit to exact numerical solutions for a variety of open cavities [11], and is also a good description of the field structure as measured in actual experimental cavities [12]. The Gaussian distribution can be written as $g(z) = \exp(-k_{||} z)^2$, where $k_{||} = 2/L_{eff}$ and L_{eff}

is determined by the shape and length of the cavity. We will use $\bar{T}(r,\theta)$ as calculated for a nontapered cavity to describe the transverse field structure under the assumption that, for a cavity operating near cutoff, any taper will be small and the dependence of $\bar{T}$ on z can be neglected.

We will also consider a uniform field, $g(z) = 1$, that extends from $z = -L/2$ to $L/2$. Such a distribution might be used to describe a long cavity in which the resonant interaction only occurs in the central part of that cavity. As in the case of the Gaussian, we will use the $\bar{T}(r,\theta)$ of a nontapered cavity.

In order to calculate the starting current and detuning, one must determine the functions F_c, F_s, $|p_o|^2$, and $G(r_e)$. For the three longitudinal field distributions discussed here, the expressions for F_c, F_s, and $|p_o|^2$, derived using Eqs. (17), (18), and (10) respectively, are given in Table I. The first column gives $g(z)$, as well as the definition of $k_{||}$ and the range of interaction between the electron beam and RF field. The sinusoidal and uniform distributions involve interactions over a finite distance L, whereas the Gaussian interaction extends from $z = -\infty$ to ∞. In the case of the uniform field, where $g(z)$ is independent of $k_{||}$, the definition of $k_{||}$ is arbitrary and does not affect the final results.

The geometric factor $G(r_e)$ and $|p_o|^2$ are calculated using Eqs. (13) and (10) respectively, where $\bar{T}(r,\theta)$ is given by Eq. (9) for a TE_{mpq} mode with a standing wave in the θ direction:

$$\bar{T}(r,\theta) = \hat{r}\left(\frac{m}{k_\perp r}\right) J_m(k_\perp r)\begin{Bmatrix}\sin m\theta\\ -\cos m\theta\end{Bmatrix} + \hat{\theta}\ \frac{1}{k_\perp}\frac{dJ_m(k_\perp r)}{dr}\begin{Bmatrix}\cos m\theta\\ \sin m\theta\end{Bmatrix}. \qquad (19)$$

Here J_m is a Bessel function of order m, and $\hat{r}$ and $\hat{\theta}$ are unit vectors. Boundary conditions yield $k_\perp = \nu_{mp}/r_w$ and $k_\parallel = q\pi/L$, where ν_{mp} is the p^{th} zero of $J'_m(x) = 0$. The brackets contain the θ dependence for the two normal modes. The geometric factor can be written as:

$$G(r_e) = \tfrac{1}{4}\left[J^2_{m-1}(k_\perp r_e) + J^2_{m+1}(k_\perp r_e)\right] \qquad \begin{matrix}\text{Standing}\\ \text{Wave}\end{matrix} \qquad (20)$$

A standing wave structure is obtained if the cylindrical (i.e.,θ) symmetry is destroyed. This can be done, for example, by cutting slots in the wall. However, for a cavity with cylindrical symmetry, the RF field structure is found to rotate in the θ direction. This has been observed in experiments [12]. For this situation, the proper description of the cross-sectional structure of the $\bar{E}$ field is:

$$\bar{T}(r,\theta) = \left[\hat{\theta}\,\frac{1}{k_\perp}\,\frac{dJ_m(k_\perp r)}{dr} \mp \hat{r}i\left(\frac{m}{k_\perp r}\right)J_m(k_\perp r)\right]\exp(\pm im\theta) \qquad (21)$$

Note that $\bar{T}$ is complex and thus $|\bar{T} \times \bar{T}^*|$ is nonzero. We have derived the linear theory for this case and found that Eqs. (14)-(18) correctly give the linear characteristics of an ECM if the following expressions for $G(r_e)$ and $|p_o|^2$ are used:

$$\begin{aligned} G(r_e) &= J^2_{m\pm1}(k_\perp r_e) \qquad \begin{matrix}\text{Rotating}\\ \text{Wave}\end{matrix} \\ |p_o|^2 &= 2|p_o|^2_{\text{standing}} \end{aligned} \qquad (22)$$

Note that the two rotating modes, designated by $\pm$, interact differently with the beam and have different $G(r_e)$ when $m \neq 0$, while $G(r_e)$ is the same for both normal modes of a standing wave structure. In this section we will use Eq. (20) to define $G(r_e)$. We will now consider some features of I_{ST} and the frequency detuning

for the case of a beam with no velocity spread, and will focus our attention on the sinusoidal and Gaussian distributions.

The sinusoidal distribution is characterized by several self-excitation regions which are dependant on q. Modes with q = 1 have the lowest starting currents, with the resonance bandwidth centered at approximately $x \simeq -1$. This observation is in agreement with the fact that the ECM interaction is a Doppler-shifted resonance that satisfies $\omega - k_{\|} u \simeq \omega_c$. Modes with $q > 1$ generally have higher starting currents because I_{ST} scales as q/Q, and Q^{-1} increases with q. One can determine the minimum value of sw^2/c^2 needed in order for emission to occur from the condition $(sw^2/c^2) > 2F_c \left(dF_c/d\dot{x}\right)^{-1}$. For a sinusoidal distribution this inequality becomes:

$$\left(\frac{sw^2}{c^2}\right) > \left[\frac{2x}{(1-x^2)} + \frac{\pi}{2} q \cot\left(\frac{(x+1)\pi q}{2}\right)\right]^{-1} \qquad (23)$$

For an ECM with a q = 1 mode operating at the minimum I_{ST} at $x \simeq -1$, sw^2/c^2 must be greater than approximately 1.5 in order for the ECM to self-oscillate. Excitation can be achieved at lower values of sw^2/c^2 by decreasing x, but this results in higher values of I_{ST}. Eq. (23) implies that the transverse energy of the electron beam must exceed a certain minimum value in order for emission to occur.

The use of a Gaussian, rather than a sinusoidal, function for g(z) can substantially alter the linear characteristics of an ECM. This can be seen in Fig. 1, where I_{ST} and the frequency detuning have been plotted for these two cases. We restrict our attention to the TE_{031} mode with $L = 10.5\lambda$ and $\omega_{031}/2\pi = 200$ GHz. We assume that the cavity has a $Q_T = 3150$ and, for copper walls, $Q_o >> Q_D$ so that the term $S/2Q_o$ can be neglected in the detuning equation. The beam,

which is assumed to have no velocity spread, interacts with the RF field at the 2nd radial maximum and has a voltage of 30kV and w/u = 1.5. Calculations are based on Eq. (16). The upper curves represent the values for I_{ST}, while the lower curves give the frequency detuning. The detuning $(\omega_\ell - \omega(\ell))$ is expressed relative to the resonance width ω_c/Q_T. For the Gaussian curves, we have assumed that $L_{eff} = L$, which is typical for an open resonator of length L with straight cylindrical walls [11]. One can see that the Gaussian resonance region is substantially narrower than that for the sine distribution, and less shifted from zero. In addition, the minimum I_{ST} for the Gaussian, which occurs at:

$$x \doteq -\left(\frac{c^2}{w^2 s}\right) - \sqrt{1 + \left(\frac{c^2}{w^2 s}\right)^2} \qquad (24)$$

or $(\omega_c - \omega_{031})\, L/\pi u \doteq -0.7$ for the parameters associated with Fig. 1, is lower by a factor of 3 than the minimum I_{ST} for a sinusoidal g(z). The degree of detuning experienced in these two cases is similar. The narrower (and less shifted) I_{ST} curve for the Gaussian can be explained primarily in terms of differences in $k_{||}$, that is, differences in the breadth of the g(z) profile. For the above example we obtain $k_{||} = 2/L = 1.21$ cm.$^{-1}$ for the Gaussian and $k_{||} = \pi/L = 1.99$ cm.$^{-1}$ for the sine. Since the wavenumber for the Gaussian is smaller, which results in a broader profile, one would expect the Doppler shift and resonance width, both of which are inversely related to the breadth of g(z), to be reduced. The lower minimum starting current for the Gaussian is also primarily a result of the lower $k_{||}$. This can be shown using Eq. (16a), which yields the following dependence for the minimum starting current with $x \approx -1$:

$$I_{ST}^{MIN} \sim k_{||}^2$$

This simple relation explains the qualitative difference between the sinusoidal and Gaussian g(z) distributions.

In order to better understand the importance of the fringe fields at each end of an open cavity, the calculation of the starting current for a Gaussian profile was redone for a finite resonant interaction extending from z = -L' to L'. In this case an analytic solution was not feasible, and the integration had to be done numerically. The results are shown in Figure 2. Here I_{ST} has been plotted for various values of L'/L. The cavity parameters given with Fig. 1 were used. The curve L'/L = ∞ is the same curve as that shown for the Gaussian in Figure 1. One can see that as L'/L decreases and less of the tails are included in the interaction region, the curves shift to more negative values of x.

Again, this effect can be explained in terms of a changing value of $k_{||}$. For $L'/L \lesssim 0.5$, the effective $k_{||}$ for the distribution is 2/L'. Thus, as L' decreases, the effective $k_{||}$ increases, increasing both the width and the shift of the resonance curve.

The general expressions derived in Section II have been compared with the results of previous studies of ECM linear theory. Chu [8] has derived the starting current for TE_{opq} modes (i.e., m = 0) with a sinusoidal longitudinal field profile and no velocity spread in the beam using a fully relativistic approach. It was found that our weakly relativistic approach agrees with his results to within 18% for a beam energy of 60 keV or less. Thus, use of a fully relativistic model introduces rather small corrections in comparison

to changes resulting from varying the RF field shape or allowing for a velocity spread in the electron beam. The results of this paper should be sufficiently accurate as long as the beam voltage is low and the device operates at the fundamental. Antakov et. al. [6] have derived the starting current for a TE_{mpq} mode with $g(z) = \sin k_{\parallel} z$ and a velocity spread in the beam. Their results were found to be in agreement with ours except for an additional factor of $(\beta_{\parallel} / \beta_{\perp})^4$ in their equation, a factor we believe is in error. Finally, our expression for I_{ST} for the Gaussian profile and no beam velocity spread was found to agree with similar results given by Nusinovich and Erm [19], as well as with an expression presented by Gaponov et. al. [12] for the minimum starting current.

IV. Beam Velocity Spread

We will now investigate the effect on I_{ST} of having a velocity spread in the electron beam. In order to avoid a detailed analysis of particle trajectories from the gun cathode, we will assume that all electrons are emitted with the same energy, and that the parallel velocity dispersion can be described by a Maxwellian with a characteristic width Δu (full width at half maximum). For simplicity, no spatial dispersion will be included. If we define $\bar{u}$ and $\bar{w}$ as the average velocities, then the electron distribution function is written as:

$$f_0(u,w) = \left(\frac{0.94}{\Delta u}\right) \exp\left(-\frac{(u-\bar{u})^2}{0.36(\Delta u)^2}\right) \delta(\bar{u}^2 + \bar{w}^2 - u^2 - w^2)(2\pi w)^{-1} \qquad (25)$$

This expression for f_o is then used in conjunction with Eq.(14) to calculate the starting current.

This calculation was done numerically for the TE_{031} mode with a sinusoidal longitudinal field distribution using the same design parameters as those given for Fig. 1. The results are shown in Fig.3, where I_{ST} has been plotted versus $\bar{x} = (\omega_c - \omega(\ell))/k_{||}\,\bar{u}$ for various velocity spreads $\Delta w/w$, which can be related to the longitudinal velocity dispersion using $\Delta u/u = (w/u)^2(\Delta w/w)$. It can be seen that large spreads in velocity have a relatively minor effect

on the minimum starting current. Increasing the velocity dispersion causes the minimum value of I_{ST} to decrease and shift towards $\bar{x} = 0$ provided the dispersion does not become excessively large. This behavior can be explained in the following manner. Let x_{opt} be that value of x at which the electrons lose the greatest fraction of their energy and I_{ST} is minimized. If an ECM with a beam velocity spread is operating at $|\bar{x}|$ slightly less than $|x_{opt}|$, then a number of electrons will have a sufficiently small velocity u such that they have an effective $x \simeq x_{opt}$. In addition, these particles will have a relatively high ratio w/u. These two factors cause these electrons to lose a larger than average fraction of their energy. It can be shown that this effect dominates, resulting in a reduction of the starting current for $|\bar{x}|$ slightly less than $|x_{opt}|$ for a beam with a velocity spread.

Although a velocity dispersion has a small and even somewhat beneficial effect in the linear regime of operation, this is not expected to be the case in the nonlinear operation of an ECM. For example, V. P. Taranenko et al. [15] conclude that a velocity spread in the electron beam has a detrimental effect on the efficiency of the device.

V. Multimode Operation

We next consider the case of multimode excitation, which is one of the major problems confronting the high power, high frequency ECM. This involves the excitation of a number of competing modes in addition to the working mode, thus adversely affecting the efficiency of the maser. This problem is exasperated as the cavity size is increased to accommodate higher powers, since one must move to higher order modes, and mode separation decreases. In order to analyze multimode excitation, the oscillation equations (6) for all possible excited modes must be solved simultaneously. In general, a mode can be excited if its frequency falls within the gain bandwidth $\Delta\omega_g \sim k_{||} u$. These equations are coupled since the perturbed current $\bar{J}$ is a function of all the modes oscillating within the cavity. Coupling between modes also occurs as a result of the ohmic losses in the cavity walls (i.e., the $Q_o^{\ell d}$ terms, where $\ell \neq d$), but these terms are typically small and can be neglected. The cross-terms associated with the $\bar{J} \cdot \bar{E}_\ell$ integral result from the fact that the RF field serves two purposes. It is responsible for the bunching of the electrons as well as the energy extraction from the electron stream. In the case of a single mode, both duties are accomplished by the same field, resulting in the geometric factor G_D being expressed in terms of $|\bar{T}(r,\theta)|^2$. In the case of multimode operation, cross-terms occur because bunching and energy extraction can be accomplished by different modes, and this gives geometric factors which are functions of $(\bar{T}_\ell \cdot \bar{T}_d^*)$ and $|\bar{T}_\ell \times \bar{T}_d^*|$, where $\bar{T}_\ell$ and $\bar{T}_d$ represent different modes.

A number of complications arise when two or more modes are allowed to oscillate within a cavity. For a single-mode analysis, the final equations for the starting current and detuning are independent of both time and RF field amplitude, which is consistent with linear theory. However, in a multimode analysis, the cross-terms associated with the interaction of two separate modes will be functions of both time and the relative amplitudes of the two modes. These terms will be proportional to $\exp(i\Delta\omega_s t)$, where $\Delta\omega_s = \omega(\ell) - \omega(d)$. The correct treatment of these terms will thus depend upon the relative frequencies of the competing modes. If $(\Delta\omega_s)^{-1}$ is small compared to the transit time of the electron in the cavity ($\tau_i \sim (k_{||} u)^{-1}$), then $\exp(i\Delta\omega_s t)$ is expected to be highly oscillatory along the electron path, mode coupling will be weak, and the cross-terms can be ignored. In this case each oscillation equation can be solved independently in the linear regime. However, if $\Delta\omega_s \leq k_{||} u$, then the cross-terms cannot be neglected, and the system of oscillation equations must be solved simultaneously. A multimode analysis would utilize Eqs.(7a) and (7b), and Eq.(11) in its generalized form. Such an analysis is beyond the scope of this paper, and will be treated in a subsequent publication. However, we will point out some of the major qualitative features of such a solution in this section.

Consider the cavity resonator treated in Section III, with a circular cross section and a thin annular beam symmetric in θ. For this cavity, we can show that two cavity modes, TE_{mpq} and

$TE_{m'p'q'}$ will only have significant competition if m = m' and p = p'. This can be explained as follows. For those competing modes with different m, the orthogonality of the θ dependence of the two modes will cause $G_D^{\ell d}$ and $G_c^{\ell d}$, $\ell \neq d$, in Eq.(11) to be zero. This will eliminate mode coupling in that case. For modes with m = m' but p $\neq$ p' (and q = q' or q $\neq$ q'), it is easy to show that the frequency difference of the modes

$$\Delta\omega_s/\omega \sim |\nu_{mp} - \nu_{mp'}|/\nu_{mp}$$

will always be quite large for modes with m or p less than about 20. Here, we have assumed a cavity near cutoff so that the q dependence of the oscillation frequency is unimportant.

Thus, in practice, mode competition in the linear theory only occurs between modes of the form TE_{mpq} and $TE_{mpq'}$. These modes can be closely spaced, particularly if q = 1 and q' = 2 and the cavity is near cutoff ($k_\perp >> k_\parallel$). Since a rigorous treatment of multimode effects is beyond the scope of this paper, we have calculated I_{ST} and the frequency detuning for closely spaced modes using the single mode equations. Therefore it should be understood that, for modes of the form TE_{mp1} and TE_{mp2} in regions of magnetic field where the starting currents for the two modes are comparable, the calculations to be presented are inaccurate.

Fig. 4 shows results for the TE_{03q} and TE_{23q} modes with q = 1 and 2. The starting current and detuning ($\omega_\ell - \omega(\ell)$) are plotted versus $x_{031} = (\omega_c - \omega_{031})/k_\parallel^{031}u$. The parameter x_{031} is effectively

a measure of the magnetic field. The device parameters are the same as those presented in conjunction with Fig. 1. Here one can see extensive mode overlap of the 031 and 032 modes. Such competition is especially prevalent in the case of gyrotrons, where $k_\perp >> k_\parallel$ and TE_{mp2} modes are very close in frequency to TE_{mp1}. In addition, the TE_{opq} and TE_{2pq} modes tend to be closely situated, especially for $p \geq 3$. The frequency detuning observed in Fig. 4 is quite small, although measurable, with $|Q_T(\omega_\ell - \omega(\ell))/\omega_c| \leq 2$ over a major portion of the I_{ST} curves.

Based on the observation that the starting current curves have an approximate width of $\Delta x \approx 2$, one can derive a simple scaling law that determines if mode competition will be a major problem. Modes TE_{mpq} and $TE_{m'p'q'}$ will not overlap when $|\omega_{mpq} - \omega_{m'p'q'}| \geq (k_\parallel + k'_\parallel)u$. Writing $k_\parallel = q\pi/L$ and $\omega_{mpq} \cong c\nu_{mp}/r_w$ gives:

$$\left| \frac{1}{8}(q + q')\Delta q\left(\frac{\lambda}{L}\right)^2 + \frac{\Delta\nu_{mp}}{\nu_{mp}} \right| \geq \frac{1}{2}(q + q')\left(\frac{u}{c}\right)\left(\frac{\lambda}{L}\right) \qquad (26)$$

as the mode separation condition, where $\Delta q = q - q'$ and $\Delta\nu_{mp} = \nu_{mp} - \nu_{m'p'}$. This is satisfied in the case of the competing TE_{031} and TE_{231} modes with $L/\lambda = 10.5$ and $\Delta\nu_{mp} = 0.2$, and thus only a slight overlap of these modes is observed in Fig. 4. However, Eq.(26) indicates competition between TE_{031} and TE_{032} ($\Delta q = 1$, $\Delta\nu_{mp} = 0$), and this is verified by the graph. Fig. 5 shows results for a shorter cavity length $L/\lambda = 5$ (vs. 10.5 in Fig. 4). Here, the starting current has been plotted versus x_{031}. At this smaller value

of L/λ, the mode separation equation (26) is not satisfied for TE_{031} and TE_{231}, and extensive overlap of these two modes is observed. The starting currents in this graph are much higher than those of Fig. 4 due primarily to the reduction of the quality factor, which scales as $Q_D \sim (L/\lambda)^2$.

VI. Conclusions

We have investigated in detail the startup characteristics of an ECM by solving the full linear theory for the device in the weakly relativistic limit. A set of analytic expressions was derived for calculating the starting current and detuning properties for any RF field distribution. The starting current was found to be simply related to the Fourier transform of the longitudinal field shape. These comprehensive results were applied to specific cases, including the sinusoidal and Gaussian distributions, which were investigated in detail. The resulting equations are fairly easy to solve, yet remain flexible enough that they can be used to study a variety of ECM problems, including velocity spread in the electron beam and mode competition.

The comparison of the sinusoidal and Gaussian distributions showed that slight alterations of the RF field longitudinal dependence can substantially change the starting current and Doppler shift associated with the resonance. In the example given, a decrease of I_{ST} by a factor of three was observed for the Gaussian vis a vis the sine case. The tails of the Gaussian were shown to cause a shift of the resonance curve.

The potential competition between modes was investigated by plotting the I_{ST} curves for a set of neighboring modes, in particular the TE_{03q} and TE_{23q} modes for $q = 1$ and 2. The starting current was calculated for each mode using the assumption that no other modes existed within the cavity. This approach was shown to be valid for our configuration

except for TE_{mpq} and $TE_{mpq'}$, modes, where $q \neq q'$. For the latter situation, the cross-terms associated with mode coupling are not negligible for those values of x that result in comparable starting currents for these two modes. For a gyrotron operating near cutoff, where $k_\perp >> k_\parallel$, there is generally extensive overlap between TE_{mpq} and $TE_{mpq'}$. However, this problem might not be severe in practice since I_{ST} increases with q and it might be possible to operate at $q = 1$ and remain below the starting regimes for $q > 1$ modes.

A velocity spread in the electron beam was found to have a small effect on the starting behavior of an ECM. Surprisingly, such a degradation of the beam caused a lowering of the minimum I_{ST}. However, it is known [15] that a velocity dispersion will have a detrimental effect on the nonlinear characteristics of the device, in particular causing the efficiency to decrease.

Calculation of the dispersion characteristics shows that the magnitude of the frequency detuning at threshold will be in the range of several times ω/Q_T as the magnetic field is varied. Since the emission bandwidth will be narrowed to less than ω/Q_T, the variation in emission frequency should be measurable. Measurement of the detuning, as well as the starting current, as a function of magnetic field could be useful in evaluating certain parameters of the ECM, such as the cavity Q.

ACKNOWLEDGMENTS

We wish to thank D. R. Cohn and L. M. Lidsky for their encouragement and support throughout this work. We also wish to thank R.C. Davidson and H.S. Uhm for their helpful discussions.

REFERENCES

1. V.A. Flyagin, A.V. Gaponov, M.I. Petelin and V.K. Yulpatov, IEEE Trans. Microwave Theory and Tech. MTT-25 (1977) 514.

2. J.L. Hirshfield and V.L. Granatstein, IEEE Trans. Microwave Theory and Tech. MTT-25 (1977) 522.

3. A.A. Andronov, V.A. Flyagin, A.V. Gaponov, A.L. Gol'denberg, M.I. Petelin, V.G. Usov and V.K. Yulpatov, Infrared Physics 18 (1978) 385. Also A.V. Gaponov, V.A. Flyagin, A.Sh. Fix, A.L. Gol'denberg, V.I. Khizhnyak, A.G. Luchinin, G.S. Nusinovich, M.I. Petelin, Sh. Ye. Tsimring, V.G. Usov, S.N. Vlasov, V.K. Yulpatov, report for the Fourth Int'l. Conf. on Infrared and Millimeter Waves and their Applications, Miami, Florida, 1979 (to be published in Int. Journal of Infrared and Millimeter Waves).

4. J.L. Hirshfield, I.B. Bernstein and J.M. Wachtel, IEEE Journal Quantum Electronics 1, No. 6 (1965) 237.

5. V.A. Zhurakhovskii and S.V. Koshevaya, Radio Eng. and Communication Systems, 10, No. 11 (1967) 71.

6. I.I. Antakov, V.S. Ergakov, E.V. Zasypkin and E.V. Sokolov, Radiophysics and Quantum Electron. 20, No. 4 (1977) 413.

7. R.S. Symons and H.R. Jory in Proceedings of the Seventh Symposium on Engineering Problems of Fusion Research (Knoxville, Tenn. 1977).

8. K.R. Chu, Phys. of Fluids 21 (1978) 2354.

9. R.J. Temkin, K. Kreischer, S.M. Wolfe, D.R. Cohn and B. Lax, Journal of Magnetism and Magnetic Materials 11 (1979) 368.

10. J.C. Slater, Microwave Electronics. D. Van Nostrand Co., New Jersey, 1950.

11. S.N. Vlasov, G.M. Zhislin, I.M. Orlova, M.I. Petelin and G.G. Rogacheva, Radiophysics and Quantum Electron. 12, No. 8 (1969) 972.

12. A.V. Gaponov, A.L. Gol'denberg, D.P. Grigor'ev, T.B. Pankratova, M.I. Petelin and V.A. Flyagin, Radiophysics and Quantum Electron. 18, No. 2 (1975) 204.

13. N.A. Krall and A.W. Trivelpiece, Principles of Plasma Physics, McGraw-Hill, Inc. 1973.

14. M.I. Petelin and V.K. Yulpatov, Radiophysics and Quantum Electron. 18 (1975) 212.

15. V.P. Taranenko, V.N. Glushenko, S.V. Koshevaya, K. Ya. Lizhdvoy, V.A. Prus and V.A. Trapezon, Elektronaya Tekhnika, Ser. 1, Elektron. SVCh, No. 12 (1974) 47.

16. M. Abramowitz and I.A. Stegun, Handbook of Mathematical Functions. Dover, New York, 1965.

17. H. Uhm, R.C. Davidson and K.R. Chu, Phys. Fluids 21, No. 10 (1978) 1877.

18. A. Yariv, Quantum Electronics. Wiley, New York, 1975.

19. G.S. Nusinovich and R.E. Erm, Elektronaya Tekhnika, Ser. 1, Elektron, SVCh, No. 8 (1972) 55.

20. J.D. Jackson, Classical Electrodynamics. Wiley, New York, 1962.

21. L.A. Vainshtein, Open Resonators and Open Waveguides, Translated from Russian by P. Beckmann, Boulder, CO., Golem Press, 1969.

TABLE I

Results for Various Longitudinal Field Distributions g(z)

g(z)	$F_c(x)$	$F_s(x)$	$\lvert p_o \rvert^2$
(1) $\sin k_{\parallel} z$ $k_{\parallel} = q\pi / L$ $0 \leq z \leq L$	$\frac{2}{(1-x^2)^2} \sin^2\left(\frac{(x+1)\pi q}{2}\right)$	$\frac{-1}{(1-x^2)^2}\left[\sin q\pi(x-1) + \frac{x(1-x^2)q\pi}{2}\right]$	$\frac{\pi L}{4} k_{\perp}^{-2}\left[\nu_{mp}^2 - m^2\right] J^2{}_m(\nu_{mp})$
(2) $e^{-k_{\parallel}^2 z^2}$ $k_{\parallel} = 2/L_{eff}$ $-\infty \leq z \leq \infty$	$\frac{\pi}{2} e^{-\frac{x^2}{2}}$	$\sqrt{\pi}\ D\left(\frac{x}{\sqrt{2}}\right)$	$(\frac{\pi}{2})^{\frac{3}{2}} \frac{L_{eff}}{2} k_{\perp}^{-2}\left[\nu_{mp}^2 - m^2\right]$ $\times\ J_m^2(\nu_{mp})$
(3) 1 $k_{\parallel} = \pi / L$ $-\frac{L}{2} \leq z \leq \frac{L}{2}$	$2\left[\frac{\sin^2 \frac{x\pi}{2}}{x^2}\right]$	$\frac{\pi}{x} - \frac{\sin(\pi x)}{x^2}$	$(\frac{\pi}{2}) L k_{\perp}^{-2}\left[\nu_{mp}^2 - m^2\right] J^2{}_m(\nu_{mp})$

$D(x) = e^{-x^2}\int_0^x e^{\alpha^2} d\alpha$ Dawson's Integral (see [16])

$\lvert p_o \rvert^2$ corresponds to a standing wave in the θ direction

Figure Captions

Fig. 1. Comparison of the linear characteristics of an ECM with a sinusoidal (S) longitudinal RF field distribution with one having a Gaussian (G) profile. Upper curves represent the starting currents, while lower curves give the frequency detuning. Cavity and beam parameters are given in the text.

Fig. 2. Variation of the starting current of an ECM with a Gaussian longitudinal profile as the range of interaction between the electron beam and RF field is changed. L is the cavity length, and L' is the interaction length. Same device parameters as for Fig. 1.

Fig. 3. Dependence of the starting current on the velocity spread of the electron beam, $\Delta w/w$, for the TE_{031} mode. ECM has RF field with sinusoidal longitudinal profile, and same operating parameters as those given for Fig. 1.

Fig. 4. Starting current (upper curves) and frequency detuning (lower curves) for the TE_{03q} and TE_{23q} modes for q = 1 and 2 and a sinusoidal longitudinal field profile. Same device parameters as for Fig. 1. A standing wave in the θ direction is assumed for the assymmetric modes.

Fig. 5. Starting current for same ECM as in Fig. 4 except cavity has been shortened to $L = 5\lambda$ (vs. 10.5λ in Fig. 4). As the ratio L/λ decreases, mode overlap becomes more pronounced.

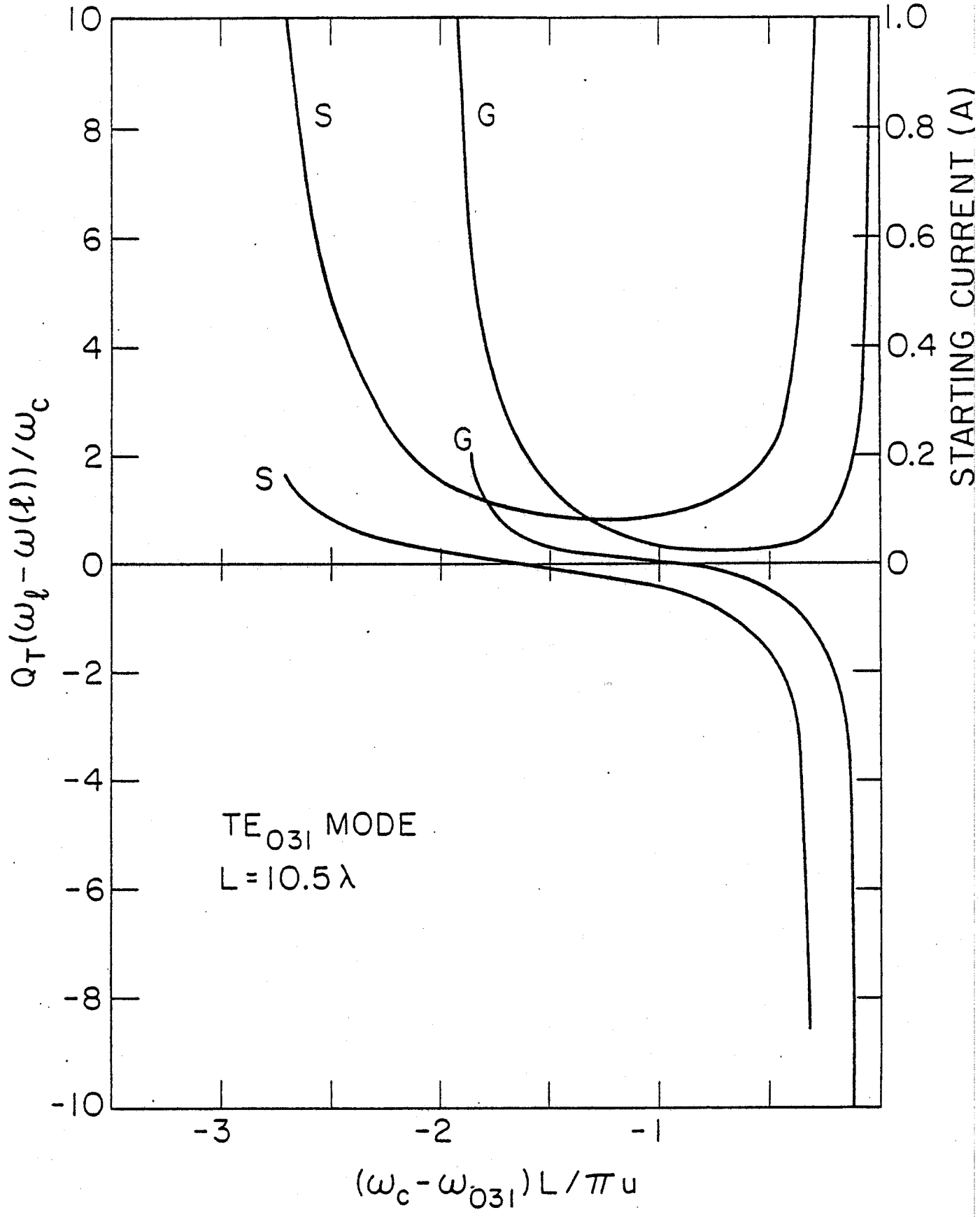
10
8
6
4
2
0
-2
-4
-6
-8
-10
-3
-2
-1
1.0
0.8
0.6
0.4
0.2
0
S
G
S
G
TE031 MODE
L = 10.5 λ
$Q_T(\omega_\ell - \omega(\ell))/\omega_c$
STARTING CURRENT (A)
$(\omega_c - \omega_{031})L/\pi u$

Fig. 1

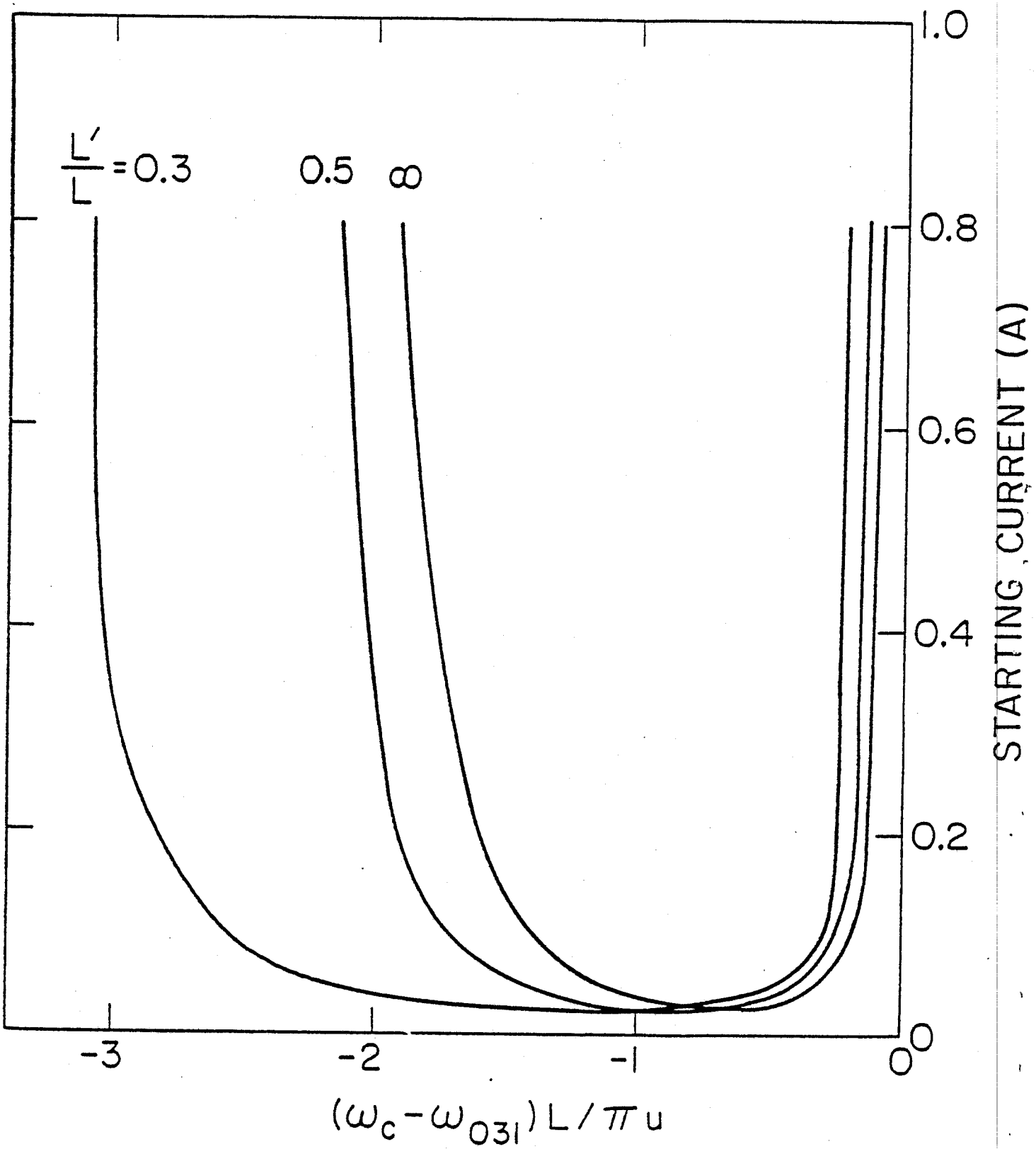
$\frac{L'}{L}$ = 0.3
0.5
∞
1.0
0.8
0.6
0.4
0.2
0
-3
-2
-1
0
STARTING CURRENT (A)
$(\omega_c - \omega_{031})\, L / \pi u$

Fig. 2

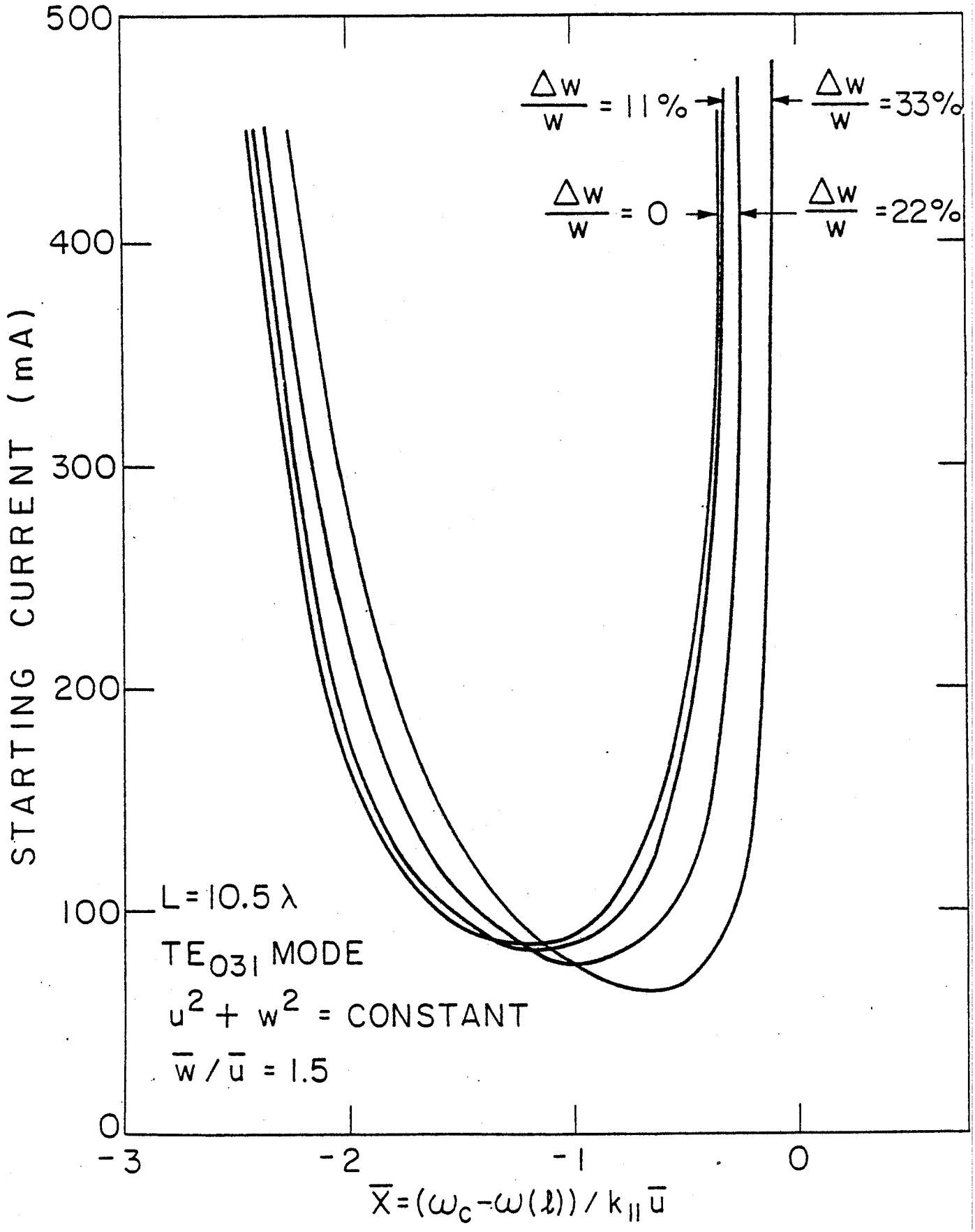
500
400
300
200
100
0
STARTING CURRENT (mA)
$\frac{\Delta w}{w}$ = 11%
$\frac{\Delta w}{w}$ =33%
$\frac{\Delta w}{w}$ = 0
$\frac{\Delta w}{w}$ =22%
L = 10.5 λ
TE031 MODE
$u^2 + w^2$ = CONSTANT
$\bar{w} / \bar{u}$ = 1.5
-3
-2
-1
0
$\bar{X} = (\omega_c - \omega(\ell)) / k_{||} \bar{u}$

Fig. 3

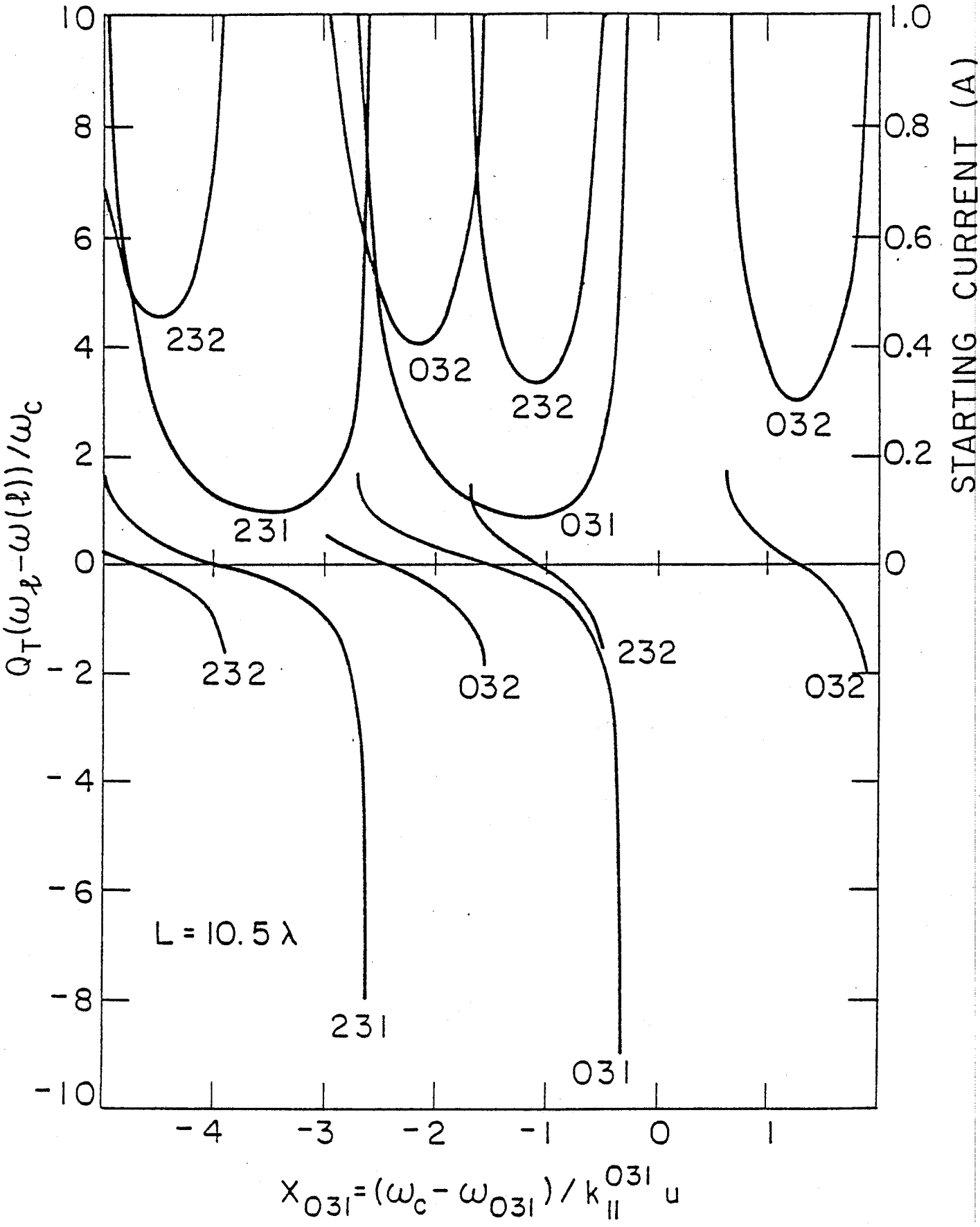
10
8
6
4
2
0
-2
-4
-6
-8
-10
1.0
0.8
0.6
0.4
0.2
0
STARTING CURRENT (A)
$Q_T(\omega_\ell - \omega(\ell))/\omega_c$
232
032
232
032
231
031
232
032
232
032
L = 10.5 λ
231
031
-4
-3
-2
-1
0
1
$X_{031} = (\omega_c - \omega_{031}) / k_{\parallel}^{031} u$

Fig. 4

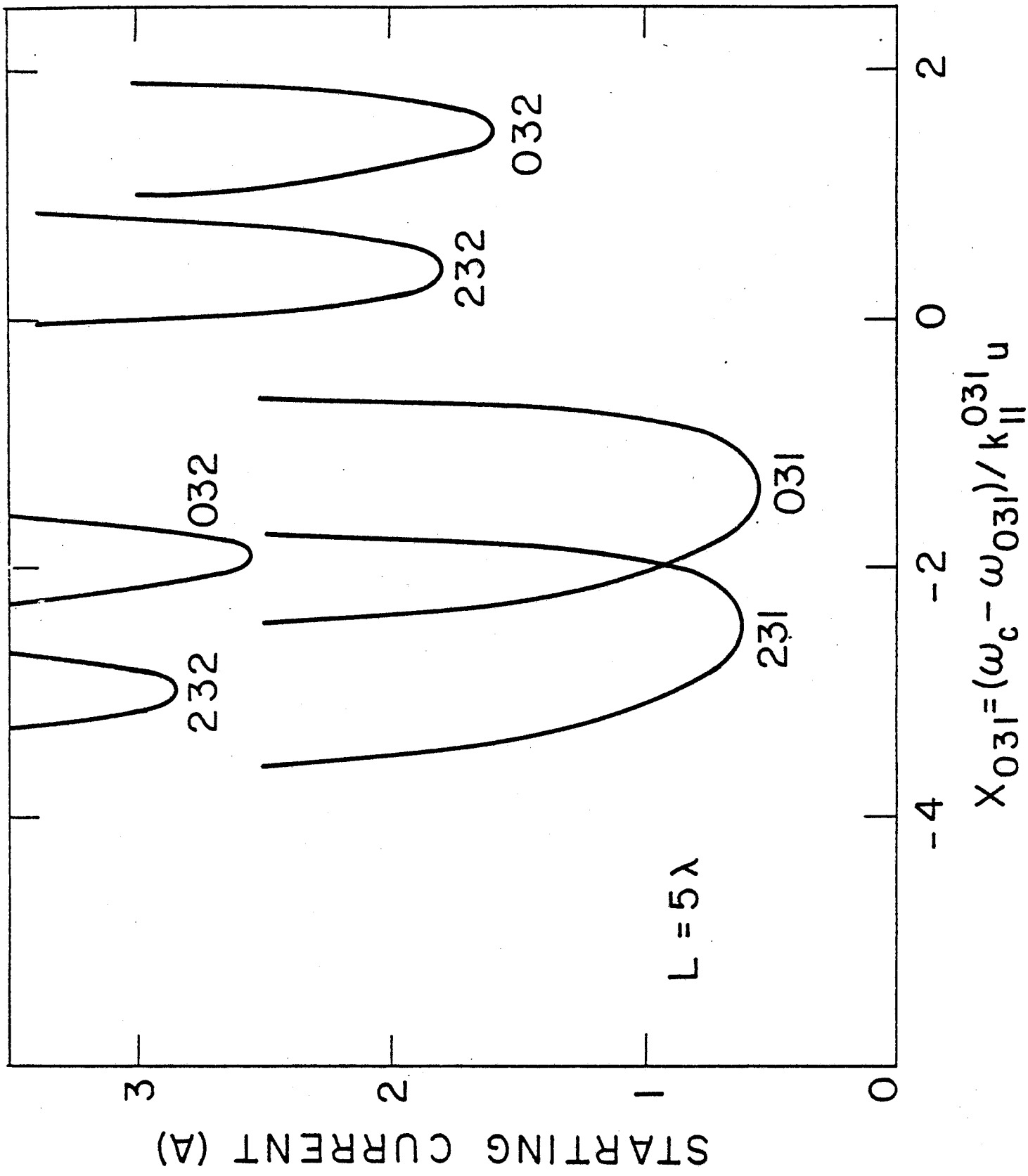
STARTING CURRENT (A)
3
2
1
0
$X_{031}=(\omega_c-\omega_{031})/k_{\parallel}^{031}u$
2
0
-2
-4
L = 5λ
032
232
031
231
032
232

Fig. 5